Progress In Electromagnetics Research, PIER 74, 141–155, 2007

FREQUENCY SELECTIVE STRUCTURES WITH STOCHASTIC DEVIATIONS

A. Karlsson and D. Sjöberg

Department of Electrical and Information Technology
Lund University
Box 118, 221 00 Lund, Sweden

B. Widenberg

Applied Composites Aktiebolag ACAB
Box 130 70, 580 13, Linköping, Sweden

Abstract—This paper deals with the performance of frequency selective structures with defects. A frequency selective structure is in this case a periodic pattern of apertures in a conducting plate. The plate can be of arbitrary thickness. The defects can be due to deviations in the placing of the apertures, in the material parameters, or in the shape of the apertures. First, the perturbation to the far-field pattern from a deviation in one aperture is analyzed. It is then shown how this affects the mean scattered power from the structure. Numerical illustrations of the perturbed fields on the structure are given.

1. INTRODUCTION

A plane Frequency Selective Structure (FSS) is a periodic structure of infinitely many identical cells. The structure acts as a filter for an incident electromagnetic plane wave. For certain frequencies the induced currents in the cells interfere constructively such that all of the incident power is transmitted through the structure, whereas waves with other frequencies are partly, or entirely, reflected. This paper presents a simple method that can handle perturbations in the periodic pattern and that can estimate the effects these perturbations have on the filtering property. The method gives the surface fields, as well as the far-fields, from the perturbed region. It is also shown

how the scattered power is affected by a stochastic distribution of perturbations.

A number of different techniques have been developed during the years to analyze unperturbed frequency selective structures. The Method of Moments (MoM), *cf.,* [6, 7], the Finite Difference Time-Domain (FDTD) technique [2], and the Finite Element Method (FEM) [1, 8], are three of the most common methods. For more complicated substrate materials, the methods in [3, 4] can be applied. The philosophy behind the perturbation method in this paper is that the numerical method and code used for the unperturbed periodic structure can, without modifications, be used to estimate the effects of perturbations to the periodic structure. Thus it is the chosen method for the unperturbed problem that sets the limits for what structures that can be handled. The methods mentioned above are very general and can *e.g.,* handle periodic patterns of metal strips, periodic patterns of apertures in conducting planes, and periodic patterns that include dielectric parts.

2. UNPERTURBED FSS

A frequency selective structure is a periodic pattern of identical cells. For simplicity it is assumed that the structure is parallel to the xy-plane and is periodic in the x-direction with a period a and in the perpendicular direction, the y-direction, with a period b. Structures that are periodic in non-perpendicular directions can be handled in the same manner, *cf.,* [8]. The FSS has a finite thickness and is assumed to occupy the region $-h < z < 0$, *cf.,* Figure 1. The FSS is assumed to be excited by an incident plane wave

$$\boldsymbol{E}^{\mathrm{i}}(\boldsymbol{r}) = \boldsymbol{E}_0 \mathrm{e}^{\mathrm{i}\boldsymbol{k}_{\mathrm{i}}\cdot\boldsymbol{r}}, \tag{1}$$

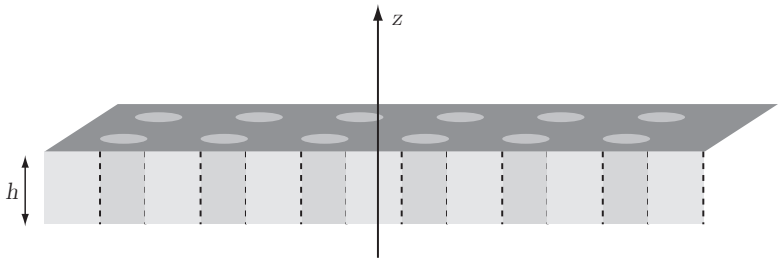

Figure 1. The frequency selective plate. The apertures may be filled with a dielectric material.

where the time dependence $\mathrm{e}^{-\mathrm{i}\omega t}$ is assumed and where $\boldsymbol{k}_i = (k_{\mathrm{i}x}, k_{\mathrm{i}y}, k_{\mathrm{i}z})$ is the wave vector. For simplicity the incident wave is assumed to be incident from below, *i.e.,* with $k_{\mathrm{i}z} > 0$. Due to the periodicity of the geometry, the reflected and transmitted fields are periodic vector functions in the x- and y-directions. The periodicity is utilized by the numerical programs and the scattering region is reduced to one cell.

3. FSS WITH A SINGLE PERTURBED CELL

If one or more cells are perturbed, a field that is not periodic will be superimposed the periodic field. This causes numerical problems since the scattering region no longer can be reduced to one cell. However, if the perturbation is small the interaction of the perturbed field with the surrounding cells can be neglected and the scattering region can be reduced to one cell. It is this approximation that makes the problem numerically feasible.

First consider an FSS where the cell S_k is perturbed, but all of the other cells are unperturbed. The total electric and magnetic fields at the surfaces of the cell are denoted $\boldsymbol{E}$, $\boldsymbol{H}$, the corresponding fields for the unperturbed case are denoted $\boldsymbol{E}^0$, $\boldsymbol{H}^0$, and the perturbation fields are denoted $\boldsymbol{E}^{\mathrm{P}}$, $\boldsymbol{H}^{\mathrm{P}}$. Thus

$$\boldsymbol{E} = \boldsymbol{E}^0 + \boldsymbol{E}^{\mathrm{P}}, \tag{2}$$

$$\boldsymbol{H} = \boldsymbol{H}^0 + \boldsymbol{H}^{\mathrm{P}}, \tag{3}$$

where the unperturbed fields are assumed to be known. The perturbation is assumed to be small enough for the following approximation to hold:

The tangential electric and magnetic surface fields on the surface of the perturbed cell are the same as the corresponding fields for an FSS where all of the cells are identical with the perturbed cell.

The approximation is referred to as the single cell approximation and is illustrated in Figure 2. The numerical examples in the numerical section indicate that this is a relevant approximation, even for quite large perturbations. There are two important features of this approximation; firstly the approximation is independent of the numerical method that is used for the solution of the scattering problem, and secondly, the perturbation is obtained by numerically solving the surface fields for two different periodic structures. A numerical method that can handle the unperturbed structure can also handle the perturbation and hence no new numerical code is needed.

In the case of a large perturbation, the single cell approximation becomes inaccurate. It is then possible to introduce supercells in order

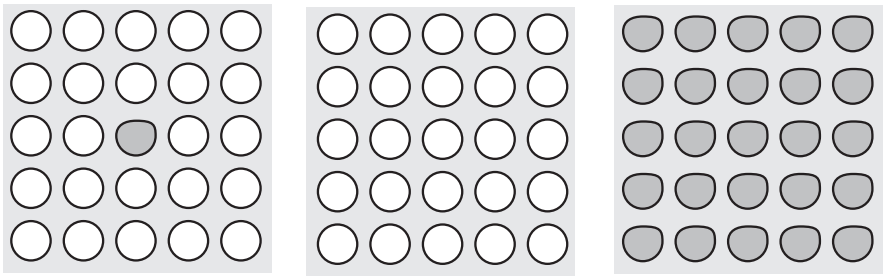

(a) (b) (c)

Figure 2. The single cell approximation. *a*) The periodic structure with one perturbed cell. *b*) The unperturbed periodic structure. *c*) The periodic structure with all of the cells perturbed. The surface field in the perturbed cell in *a* is approximately the same as the surface field in the corresponding cell in *c*. The perturbation of the surface field in the perturbed cell is approximately the difference between the surface fields in the corresponding cells in *c* and *b*.

to obtain the perturbed fields. A supercell is depicted in Figure 3. It consists of the perturbed cell and at least one of the cells surrounding the perturbed cell. To obtain the perturbation to the field, one creates a periodic structure of supercells. The perturbed surface field of the perturbed cell is given by $\boldsymbol{E}^{\mathrm{P}} = \boldsymbol{E} - \boldsymbol{E}^{0}$, where in this case $\boldsymbol{E}$ is the surface field from the periodic structure with each cell being a supercell. The supercells can be handled by an FDTD program for periodic structures without modification. Methods based on FEM or on MoM have to be slightly modified. In Appendix A it is seen how a method based on FEM is modified to handle supercells. Obviously the numerical calculations with supercells are more CPU-time consuming than without supercells. By comparing the single cell calculation with a supercell calculation, a good estimate of the error can be obtained. In the rest of the paper the approximation based on supercells is referred to as the supercell approximation, in contrast to the single cell approximation.

4. FSS WITH SEVERAL PERTURBED CELLS

Now consider an FSS with more than one perturbed cell. If the perturbed cells are densely distributed, then if the supercell approximation is used, all of the cells in the supercell should be unaltered and a periodic structure with that supercell is formed, *cf.,*

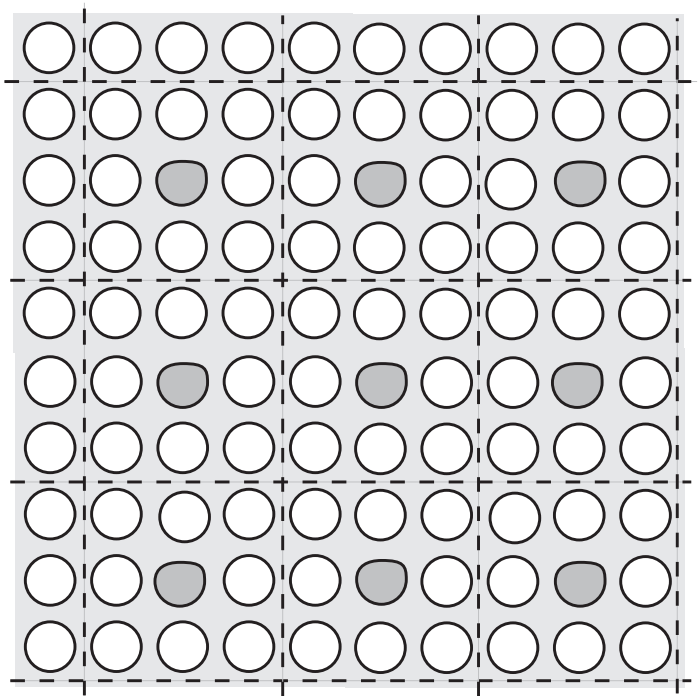

Figure 3. The supercell approximation. The surface field in the perturbed cell in the structure in Figure 2 is approximately the same as the surface field in the corresponding cell in the above structure. The approximation obtained from the supercell structure is better than the one obtained from the single cell approximation, *cf.,* Figure 2.

Figure 4. Otherwise, if the perturbed cells are sparsely distributed and it is unlikely that two neighboring cells are perturbed, supercells where the other cells are unperturbed are accurate. When the perturbed cells have stochastic variations and when their distribution is stochastic the methods described in [5] and Section 7 are applicable.

5. FAR-FIELD AMPLITUDE

The perturbation of the far-field can be determined from the integral representation of the field. The perturbation to the far-field from one perturbed cell yields

$$\boldsymbol{E}_{\mathrm{s}}(\boldsymbol{r}) = \frac{\mathrm{e}^{\mathrm{i}kr}}{kr}\boldsymbol{F}(\hat{\boldsymbol{r}}). \tag{4}$$

The far-field amplitude is different above and below the FSS. In both cases the expression for the perturbation reads

$$\boldsymbol{F}^{\mathrm{P}}(\hat{\boldsymbol{r}}) = \mathrm{i}\frac{k^2}{4\pi}\hat{\boldsymbol{r}} \times \iint_{S_k} [\hat{\boldsymbol{n}} \times \boldsymbol{E}^{\mathrm{P}}(\boldsymbol{r}') - \eta_0 \hat{\boldsymbol{r}} \times (\hat{\boldsymbol{n}} \times \boldsymbol{H}^{\mathrm{P}}(\boldsymbol{r}'))]\mathrm{e}^{-\mathrm{i}k\hat{\boldsymbol{r}}\cdot\boldsymbol{r}'}\,\mathrm{d}S'. \tag{5}$$

For the far-field above the FSS ($z > 0$), S_k is the surface of the cell at $z = 0$ and $\hat{\boldsymbol{n}} = \hat{\boldsymbol{z}}$, and for the far-field below the FSS ($z < -h$), S_k is the surface of the cell at $z = -h$ and $\hat{\boldsymbol{n}} = -\hat{\boldsymbol{z}}$.

From this expression it is seen that the far field is essentially a Fourier transform of the spatial distribution of the tangential electric and magnetic fields. This means that if the perturbed fields are non-zero only in a very small region, they will affect many scattering directions $\hat{\boldsymbol{r}}$, since the Fourier transform of a function with small support always has large support. This is the origin of diffuse scattering from the perturbed FSS; the unperturbed FSS only scatters in the specular directions, whereas the perturbed FSS scatters in all directions (albeit with a small amplitude). This also reduces the polarization sensitivity of an FSS.

6. TRANSLATED APERTURE

The simplest case of perturbation is a displacement of the cell number p by a vector $\delta\boldsymbol{r}_p = (\delta x_p, \delta y_p, 0)$. The displacement is assumed to be small enough for the single cell approximation to hold. The difference between the case with all of the apertures displaced and the case with no cells displaced is simply due to the translation of the coordinate system. The surface fields of the displaced cell are given by

$$\boldsymbol{E}_{\mathrm{T}}(\boldsymbol{r}) = \mathrm{e}^{\mathrm{i}\boldsymbol{k}_{\mathrm{i}}\cdot\delta\boldsymbol{r}_p}\boldsymbol{E}^0_{\mathrm{T}}(\boldsymbol{r}), \tag{6}$$

$$\boldsymbol{H}_{\mathrm{T}}(\boldsymbol{r}) = \mathrm{e}^{\mathrm{i}\boldsymbol{k}_{\mathrm{i}}\cdot\delta\boldsymbol{r}_p}\boldsymbol{H}^0_{\mathrm{T}}(\boldsymbol{r}), \tag{7}$$

where again $\boldsymbol{E}^0_{\mathrm{T}}$ and $\boldsymbol{H}^0_{\mathrm{T}}$ are the tangential field for the unperturbed cell. The corresponding perturbations to the surface fields are

$$\boldsymbol{E}^{\mathrm{P}}_{\mathrm{T}}(\boldsymbol{r}) = (\mathrm{e}^{\mathrm{i}\boldsymbol{k}_{\mathrm{i}}\cdot\delta\boldsymbol{r}_p} - 1)\boldsymbol{E}^0_{\mathrm{T}}(\boldsymbol{r}), \tag{8}$$

$$\boldsymbol{H}^{\mathrm{P}}_{\mathrm{T}}(\boldsymbol{r}) = (\mathrm{e}^{\mathrm{i}\boldsymbol{k}_{\mathrm{i}}\cdot\delta\boldsymbol{r}_p} - 1)\boldsymbol{H}^0_{\mathrm{T}}(\boldsymbol{r}). \tag{9}$$

The far-field amplitude is given by

$$\boldsymbol{F}(\hat{\boldsymbol{r}}) = \mathrm{e}^{\mathrm{i}\boldsymbol{q}\cdot\delta\boldsymbol{r}_p}\boldsymbol{F}^0(\hat{\boldsymbol{r}}), \tag{10}$$

where $\boldsymbol{F}^0$ is the far-field amplitude for a cell that is not translated and where

$$\boldsymbol{q} = \boldsymbol{k}_\mathrm{i} - k\hat{\boldsymbol{r}}. \tag{11}$$

Hence k is the wave number and $\hat{\boldsymbol{r}} = \boldsymbol{r}/r$. In all directions where $\boldsymbol{q}\cdot\delta\boldsymbol{r}_p = n2\pi$ the perturbation to the far-field is zero. Since $\delta\boldsymbol{r}_p$ is small this only happens for $n = 0$, *i.e.,* in the forward direction ($\boldsymbol{k}_i - k\hat{\boldsymbol{r}} = \boldsymbol{0}$) and in the specular reflection direction, $k\hat{\boldsymbol{r}} = (k_{ix}, k_{iy}, -k_{iz})$. If the first order term in powers of δ is kept, it is seen that

$$\boldsymbol{E}^\mathrm{P}_\mathrm{T}(\boldsymbol{r}) = \mathrm{i}(\boldsymbol{k}_\mathrm{i}\cdot\delta\boldsymbol{r}_p)\boldsymbol{E}^0_\mathrm{T}(\boldsymbol{r}), \tag{12}$$

$$\boldsymbol{H}^\mathrm{P}_\mathrm{T}(\boldsymbol{r}) = \mathrm{i}(\boldsymbol{k}_\mathrm{i}\cdot\delta\boldsymbol{r}_p)\boldsymbol{H}^0_\mathrm{T}(\boldsymbol{r}), \tag{13}$$

$$\boldsymbol{F}^\mathrm{P}(\hat{\boldsymbol{r}}) = \mathrm{i}(\boldsymbol{q}\cdot\delta\boldsymbol{r}_p)\boldsymbol{F}^0(\hat{\boldsymbol{r}}). \tag{14}$$

The perturbations to the far-field in the forward direction and in the specular reflection direction are of second order in $\delta\boldsymbol{r}_p$ and can not be obtained by retaining only terms linear in δ. Since the perturbed far-field is proportional to the unperturbed far-field, this demonstrates that (to first order) the polarization sensitivity of the FSS is not affected by pure translations of the apertures.

7. SCATTERED POWER

From the previous analysis we see that, at least to first order, the perturbed fields are proportional to the perturbation $\delta\boldsymbol{r}_p$. This means that if we take the mean value of many perturbations with zero mean, the perturbed field is zero. However, for any random variable X with zero mean, $\langle X\rangle = 0$, and probability density $f_X(x)$, we have

$$\left\langle X^2\right\rangle = \int x^2 f_X(x)\,\mathrm{d}x \neq 0. \tag{15}$$

since the probability density satisfies $f_X(x) \geq 0$ for all outcomes x. This means that even though the mean perturbed far field is zero, $\left\langle \boldsymbol{F}^\mathrm{P}\right\rangle = \boldsymbol{0}$, it still carries some energy, corresponding to the mean of the square of the far field, $\left\langle |\boldsymbol{F}^\mathrm{P}|^2\right\rangle$. In [5], the scattered power is computed using the scattered power per unit solid angle,

$$U_s(\hat{\boldsymbol{r}}) = \frac{1}{2\eta_0}\left\langle r^2|\boldsymbol{E}_\mathrm{s}(\boldsymbol{r})|^2\right\rangle, \tag{16}$$

and the incident power,

$$P_\mathrm{i} = \frac{1}{2\eta_0}|\boldsymbol{E}_0|^2 NA|\hat{\boldsymbol{k}}_\mathrm{i}\cdot\hat{\boldsymbol{z}}|. \tag{17}$$

The corresponding power scattering coefficient per unit solid angle (differential scattering cross section) for an infinite structure is then

$$\frac{U_s(\hat{\boldsymbol{r}})}{P_{\mathrm{i}}} = \frac{1}{k^2 A|\hat{\boldsymbol{k}}_{\mathrm{i}} \cdot \hat{\boldsymbol{z}}|} \left(\frac{\left\langle |\boldsymbol{F}^{\mathrm{P}}(\hat{\boldsymbol{r}})|^2 \right\rangle}{|\boldsymbol{E}_0|^2} + \frac{|\boldsymbol{F}^0(\hat{\boldsymbol{r}})|^2}{|\boldsymbol{E}_0|^2} 4\pi^2 \delta_{\mathrm{D}}(q_x)\delta_{\mathrm{D}}(q_y) \right), \tag{18}$$

where $\boldsymbol{F}^0(\hat{\boldsymbol{r}})$ is the far-field amplitude for one cell of the unperturbed structure, and we assume that the perturbed far field $\boldsymbol{F}^{\mathrm{P}}(\hat{\boldsymbol{r}})$ has zero mean, $\langle \boldsymbol{F}_{\mathrm{P}} \rangle = \boldsymbol{0}$. Since we already use the symbol δ for perturbations, the Dirac delta functions in the last term have been denoted $\delta_{\mathrm{D}}(q_x)$ and $\delta_{\mathrm{D}}(q_y)$. Their occurrence indicates that this term contributes only in the specular directions, defined by $\boldsymbol{q}_{xy} = \boldsymbol{k}_{\mathrm{i},xy} - k\hat{\boldsymbol{r}}_{xy} = \boldsymbol{0}$, or $k\hat{\boldsymbol{r}} = (k_{\mathrm{i},x}, k_{\mathrm{i},y}, \pm k_{\mathrm{i},z})$.

In the case where the perturbations are due to zero-mean translations $\delta\boldsymbol{r}_n = (\delta x_n \delta y_n, 0)$, assumed much smaller than the wavelength so that $|\boldsymbol{q} \cdot \delta\boldsymbol{r}_n| \ll 1$, this simplifies to

$$\frac{U_s(\hat{\boldsymbol{r}})}{P_{\mathrm{i}}} = \frac{|\boldsymbol{F}^0(\hat{\boldsymbol{r}})|^2}{k^2 A|\boldsymbol{E}_0|^2|\hat{\boldsymbol{k}}_{\mathrm{i}} \cdot \hat{\boldsymbol{z}}|} \Big\{ (q_x^2 + q_y^2)\delta^2 + 4\pi^2 \delta_{\mathrm{D}}(q_x)\delta_{\mathrm{D}}(q_y) \Big\}, \tag{19}$$

where $\delta^2 = \left\langle |\delta\boldsymbol{r}|^2 \right\rangle$ is the variance of the translations. From this expression it is clearly seen that the first term inside the curly brackets represent a diffuse scattering, *i.e.,* power is scattered in directions other than the specular directions.

8. NUMERICAL EXAMPLES

In this section it is indicated that the perturbed surface fields are localized fields that in most cases are negligible in the cells surrounding the perturbed cell. This is done by calculating the perturbation to the tangential electric and magnetic fields on the surface of the perturbed cell, using the single cell approximation. In this case the unperturbed cell consists of a circular aperture in a perfectly conducting plate. The thickness of the plate is 1 mm, the radius of the aperture is 15 mm, the cell is quadratic 23×23 mm, and the center of the aperture coincides with the center of the cell. The incident electric field is a linearly polarized plane wave at normal incidence, with the electric field in the x-direction, *i.e.,* the horizontal direction in the figure. The frequency is 10 GHz. The perturbed cell has its aperture displaced either a distance 4 mm to the right or 4 mm upwards.

The surface fields were calculated by a method that utilizes FEM in combination with a mode matching technique, *cf.,* [8]. The

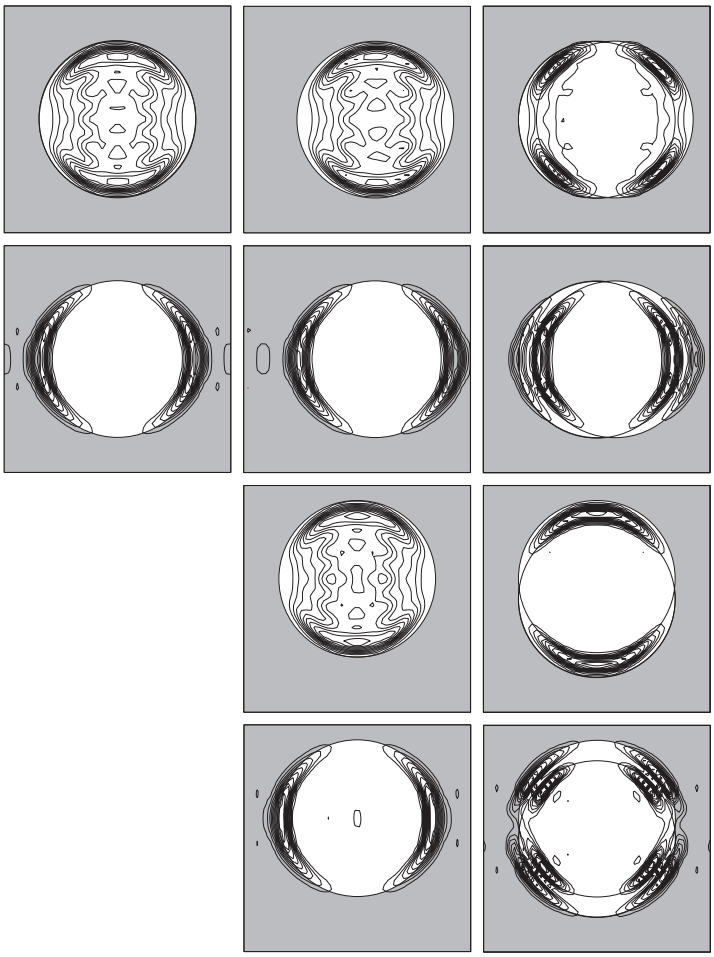

Figure 4. The surface fields of the tangential electric and magnetic fields of cells with circular apertures. The incident field, the geometry, and the figures are described in Section 8.

perturbed fields, $\boldsymbol{E}_{\mathrm{T}}^{\mathrm{P}}(\boldsymbol{r})$ and $\boldsymbol{H}_{\mathrm{T}}^{\mathrm{P}}(\boldsymbol{r})$, were obtained by first solving the unperturbed periodic case to get $\boldsymbol{E}_{\mathrm{T}}^{0}(\boldsymbol{r})$ and $\boldsymbol{H}_{\mathrm{T}}^{0}(\boldsymbol{r})$, and then solving the periodic case with all cells displaced to obtain $\boldsymbol{E}_{\mathrm{T}}(\boldsymbol{r})$ and $\boldsymbol{H}_{\mathrm{T}}(\boldsymbol{r})$. It was checked that the latter fields only differ by a phase shift $\boldsymbol{k} \cdot \delta\boldsymbol{r}$ compared to the unperturbed fields, *cf.,* Subsection 6. The resulting fields, $\boldsymbol{E}_{\mathrm{T}}^{\mathrm{P}}(\boldsymbol{r})$ and $\boldsymbol{H}_{\mathrm{T}}^{\mathrm{P}}(\boldsymbol{r})$, are shown in Figure 4. Let (i, j) denote the subfigure in row i and column j. The unperturbed tangential electric field $\boldsymbol{E}_{\mathrm{T}}^{0}$ is shown in figure (1,1) and the corresponding magnetic field

$\boldsymbol{H}_{\mathrm{T}}^{0}$ in figure (2,1). In figures (1,2) and (2,2) the tangential electric and magnetic fields $\boldsymbol{E}_{\mathrm{T}}$ and $\boldsymbol{H}_{\mathrm{T}}$ are shown for the periodic case with all of the apertures displaced horizontally a vector $\delta\boldsymbol{r} = \delta x\hat{\boldsymbol{x}}$, with $\delta x = 4\,\mathrm{mm}$. The perturbation to the tangential electric and magnetic fields, $\boldsymbol{E}_{\mathrm{T}}^{\mathrm{P}}$ and $\boldsymbol{H}_{\mathrm{T}}^{\mathrm{P}}$, are shown in figures (1,3) and (2,3), respectively. The case with a perturbation $\delta\boldsymbol{r} = \delta y\hat{\boldsymbol{y}}$ with $\delta y = 4\,\mathrm{mm}$ is shown in figures (3,2), (3,3), (4,2), and (4,4). Then the figures (3,2) and (4,2) depict the electric and magnetic fields for the periodic case with all of the apertures displaced and figures (4,2) and (4,3) depict the perturbations to the tangential electric and magnetic fields.

As seen from the plots in Figure 4, the perturbation of the fields are concentrated to the area close to the edge of the aperture. The perturbation is close to zero at the border between the cells. Due to (18), the effect of these perturbations do not appear primarily in the reflection and transmission coefficients, but in a diffuse scattering in the non-specular scattering directions.

It is anticipated that the perturbation to the surface fields are negligible in the other cells. This can be checked by calculations using supercells, the method of which is described in Appendix A.

9. CONCLUSIONS

A manufactured frequency selective structure will always deviate slightly from a perfect periodic structure. This paper presents a procedure to estimate the deterioration of the desired performance of the structure, focussing on the change of tangential electric and magnetic fields. The procedure utilizes numerical methods that are developed for perfect periodic structures. This is an advantage since only a small amount of new code has to be written. The procedure gives possibilities to choose the level of accuracy of the numerical calculations. This is done by the introduction of supercells that consist of several individual cells.

ACKNOWLEDGMENT

The Swedish Defence Materiel Administration (FMV) is gratefully acknowledged for financial support.

APPENDIX A. SUPERCELLS

In [8] a method that can handle frequency selective structures with apertures was described. The method is based on FEM and expansions in Floquet modes. The drawback is that the method can only handle

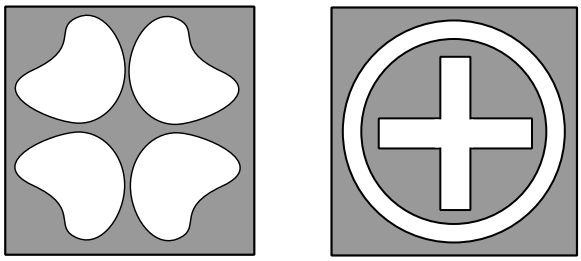

(a) (b)

Figure A1. Two examples of unit cells that contain more than one aperture: (a) Four apertures. (b) Two apertures: an annular and a crossed dipole aperture.

cells with a single aperture. In this appendix it is shown how the method can be generalized to handle supercells.

Consider a frequency selective structure where the unit cell contains M apertures $\Omega_1, \Omega_2, \ldots, \Omega_M$. An example of such a cell with two different apertures; Ω_1 as an annular aperture, and Ω_2 as a a crossed dipole aperture, is given in Figure A1. The structure may contain dielectric layers on both sides of the metallic plate. In the regions outside the structure and in the dielectric layers, the fields are expanded in Floquet modes, whereas in the apertures the fields are expanded in waveguide modes. For general structures these modes are determined numerically by FEM. The waveguide mode amplitudes and the amplitudes for the Floquet modes are related to each other by scattering matrices. In this appendix it is shown how the scattering matrix between the waveguide mode amplitudes and the Floquet mode amplitudes in an adjacent dielectric layer can be obtained.

The fields inside the dielectric layer are expanded in Floquet modes

$$\boldsymbol{E}^{\mathrm{a}}_{\mathrm{T}}(\boldsymbol{r}) = \sum_{lmn} (a^{+}_{lmn} \mathrm{e}^{\mathrm{i}\gamma^{\mathrm{a}}_{mn} z} + a^{-}_{lmn} \mathrm{e}^{-\mathrm{i}\gamma^{\mathrm{a}}_{mn} z}) \boldsymbol{R}^{\mathrm{a}}_{\mathrm{T}lmn}(\boldsymbol{\rho}), \tag{A1}$$

$$\boldsymbol{H}^{\mathrm{a}}_{\mathrm{T}}(\boldsymbol{r}) = \sum_{lmn} (a^{+}_{lmn} \mathrm{e}^{\mathrm{i}\gamma^{\mathrm{a}}_{mn} z} - a^{-}_{lmn} \mathrm{e}^{-\mathrm{i}\gamma^{\mathrm{a}}_{mn} z}) \boldsymbol{T}^{\mathrm{a}}_{\mathrm{T}lmn}(\boldsymbol{\rho}). \tag{A2}$$

The explicit expressions for the Floquet modes $\boldsymbol{R}^{\mathrm{a}}_{\mathrm{T}lmn}$ and $\boldsymbol{T}^{\mathrm{a}}_{\mathrm{T}lmn}$ are given in [8]. The fields inside the apertures are expanded in waveguide

modes. In aperture Ω_i the expansion is

$$\boldsymbol{E}_{\mathrm{T}}^{\mathrm{b}i}(\boldsymbol{r}) = \sum_{vn} (b_{vn}^{i+} \mathrm{e}^{\mathrm{i}k_{zn}^{\mathrm{b}i} z} + b_{vn}^{i-} \mathrm{e}^{-\mathrm{i}k_{zn}^{\mathrm{b}i} z}) \boldsymbol{E}_{\mathrm{T}vn}^{\mathrm{b}i}(\boldsymbol{\rho}), \tag{A3}$$

$$\boldsymbol{H}_{\mathrm{T}}^{\mathrm{b}i}(\boldsymbol{r}) = \sum_{vn} (b_{vn}^{i+} \mathrm{e}^{\mathrm{i}k_{zn}^{\mathrm{b}i} z} - b_{vn}^{i-} \mathrm{e}^{-\mathrm{i}k_{zn}^{\mathrm{b}i} z}) \boldsymbol{H}_{\mathrm{T}vn}^{\mathrm{b}i}(\boldsymbol{\rho}), \tag{A4}$$

where the waveguide modes $\boldsymbol{E}_{\mathrm{T}vn}^{\mathrm{b}i}(\boldsymbol{\rho})$ are an orthonormal set of vector waves, *cf.,* [8].

At the interface $z = z_0$ the tangential electric field is continuous over the entire interface D, while the magnetic field is continuous over the apertures, *i.e.,* the boundary conditions read

$$\boldsymbol{E}_{\mathrm{T}}^{\mathrm{a}}(\boldsymbol{\rho}, z_0) = \begin{cases} \boldsymbol{E}_{\mathrm{T}}^{\mathrm{b}i}(\boldsymbol{\rho}, z_0), & \boldsymbol{\rho} \in \Omega_i, i = 1, 2, \ldots, N, \\ \boldsymbol{0}, & \boldsymbol{\rho} \in D \setminus (\Omega_1 \cup \Omega_2 \cup \ldots \cup \Omega_N), \end{cases} \tag{A5}$$

$$\boldsymbol{H}_{\mathrm{T}}^{\mathrm{a}}(\boldsymbol{\rho}, z_0) = \boldsymbol{H}_{\mathrm{T}}^{\mathrm{b}i}(\boldsymbol{\rho}, z_0), \quad \boldsymbol{\rho} \in \Omega_i, i = 1, 2, \ldots, N. \tag{A6}$$

Introducing

$$A_{lmn}^{\pm}(z) = a_{lmn}^{\pm} \mathrm{e}^{\pm \mathrm{i}\gamma_{mn}^{\mathrm{a}} z}, \tag{A7}$$

$$B_{vn}^{i\pm}(z) = b_{vn}^{i\pm} \mathrm{e}^{\pm \mathrm{i}k_{zn}^{\mathrm{b}i} z}, \tag{A8}$$

and enforcing the continuity condition of the fields at the interface $z = z_0$ yield

$$\sum_{lmn} (A_{lmn}^{+}(z_0) + A_{lmn}^{-}(z_0)) \boldsymbol{R}_{\mathrm{T}lmn}^{\mathrm{a}}(\boldsymbol{\rho}) = \begin{cases} \sum_{vn} (B_{vn}^{i+}(z_0) + B_{vn}^{i-}(z_0)) \boldsymbol{E}_{\mathrm{T}vn}^{\mathrm{b}i}(\boldsymbol{\rho}), & \boldsymbol{\rho} \in \Omega_i, \\ \boldsymbol{0}, & \boldsymbol{\rho} \in D \setminus (\Omega_1 \cup \Omega_2 \cup \ldots \cup \Omega_N), \end{cases} \tag{A9}$$

and

$$\sum_{lmn} (A_{lmn}^{+}(z_0) - A_{lmn}^{-}(z_0)) \boldsymbol{T}_{\mathrm{T}lmn}^{\mathrm{a}}(\boldsymbol{\rho}) = \sum_{vn} (B_{vn}^{i+}(z_0) - B_{vn}^{i-}(z_0)) \boldsymbol{H}_{\mathrm{T}vn}^{\mathrm{b}i}(\boldsymbol{\rho}), \quad \boldsymbol{\rho} \in \Omega_i. \tag{A10}$$

To obtain a linear system of equations for the coefficients, the inner product is taken between (A9) and $\boldsymbol{T}_{\mathrm{T}l'm'n'}^{\mathrm{a}*}$, and between (A10) and

$\boldsymbol{E}^{\mathrm{bi}*}_{\mathrm{T}v'n'}$, $i = 1, 2, \ldots, N$. The inner product integrals are

$$\begin{aligned}
\mathbf{R}_{lmn,l'm'n'} &= \int_D \hat{z} \cdot (\boldsymbol{R}^{\mathrm{a}}_{\mathrm{T}lmn} \times \boldsymbol{T}^{\mathrm{a}*}_{\mathrm{T}l'm'n'})\,\mathrm{d}S \\
&= \int_D \boldsymbol{R}^{\mathrm{a}}_{\mathrm{T}lmn} \cdot (\boldsymbol{T}^{\mathrm{a}*}_{\mathrm{T}l'm'n'} \times \hat{z})\,\mathrm{d}S \\
&= \frac{Y^{\mathrm{a}*}_{l'm'n'}}{\eta_0} \int_D (\boldsymbol{R}^{\mathrm{a}}_{\mathrm{T}lmn} \cdot \boldsymbol{R}^{\mathrm{a}*}_{\mathrm{T}l'm'n'})\,\mathrm{d}S \\
&= \frac{Y^{\mathrm{a}*}_{lmn}}{\eta_0} \delta_{ll'}\delta_{mm'}\delta_{nn'}, \qquad \text{(A11)} \\
\mathbf{Q}^i_{vn,v'n'} &= \int_{\Omega_i} \hat{z} \cdot (\boldsymbol{E}^{\mathrm{bi}}_{\mathrm{T}vn} \times \boldsymbol{H}^{\mathrm{bi}*}_{\mathrm{T}v'n'})\,\mathrm{d}S = \frac{Y^{\mathrm{bi}*}_{vn}}{\eta_0}\delta_{vv'}\delta_{nn'}, \qquad \text{(A12)}
\end{aligned}$$

and

$$\begin{aligned}
\mathbf{C}^i_{vn,l'm'n'} = \int_{\Omega_i} \hat{z}\cdot(\boldsymbol{E}^{\mathrm{bi}}_{\mathrm{T}vn}\times\boldsymbol{T}^{\mathrm{a}*}_{\mathrm{T}l'm'n'})\,\mathrm{d}S &= \int_{\Omega_i} \boldsymbol{E}^{\mathrm{bi}}_{\mathrm{T}vn}\cdot(\boldsymbol{T}^{\mathrm{a}*}_{\mathrm{T}l'm'n'}\times\hat{z})\,\mathrm{d}S \\
&= \frac{Y^{\mathrm{a}*}_{l'm'n'}}{\eta_0} \int_{\Omega_i} (\boldsymbol{E}^{\mathrm{bi}}_{\mathrm{T}vn} \cdot \boldsymbol{R}^{\mathrm{a}*}_{\mathrm{T}l'm'n'})\,\mathrm{d}S, \qquad \text{(A13)}
\end{aligned}$$

where D is the entire surface of the cell. With these definitions, the linear system for the coefficients is

$$\begin{cases}
\mathbf{R}(\boldsymbol{A}^+ + \boldsymbol{A}^-) = \sum_i \mathbf{C}^t_i(\boldsymbol{B}^+_i + \boldsymbol{B}^-_i), \\
\mathbf{C}^*_i(\boldsymbol{A}^+ - \boldsymbol{A}^-) = \mathbf{Q}^*_i(\boldsymbol{B}^+_i - \boldsymbol{B}^-_i), \quad i = 1, 2, \ldots, N,
\end{cases} \qquad \text{(A14)}$$

The matrices $\mathbf{R}$ and $\mathbf{Q}_i$ are quadratic, but the matrix $\mathbf{C}_i$ is not necessarily quadratic. The linear system is rewritten as

$$\begin{cases}
\boldsymbol{A}^- = \sum_i \mathbf{R}^{-1}\mathbf{C}^t_i(\boldsymbol{B}^+_i + \boldsymbol{B}^-_i) - \boldsymbol{A}^+, \\
\boldsymbol{B}^+_i = \mathbf{Q}^{*-1}_i\mathbf{C}^*_i(\boldsymbol{A}^+ - \boldsymbol{A}^-) + \boldsymbol{B}^-_i \quad i = 1, 2, \ldots, N.
\end{cases} \qquad \text{(A15)}$$

The lower expression is inserted in the upper expression in (A14). This gives

$$\begin{aligned}
\mathbf{R}(\boldsymbol{A}^+ + \boldsymbol{A}^-) = \sum_i [\mathbf{C}^t_i\mathbf{Q}^{*-1}_i\mathbf{C}^*_i(\boldsymbol{A}^+ - \boldsymbol{A}^-) + 2\mathbf{C}^t_i\boldsymbol{B}^-_i] \;\Leftrightarrow \\
(\mathbf{R} + \sum_i \mathbf{C}^t_i\mathbf{Q}^{*-1}_i\mathbf{C}^*_i)\boldsymbol{A}^- = -(\mathbf{R} - \sum_i \mathbf{C}^t_i\mathbf{Q}^{*-1}_i\mathbf{C}^*_i)\boldsymbol{A}^+ + 2\sum_i \mathbf{C}^t_i\boldsymbol{B}^-_i
\end{aligned} \qquad \text{(A16)}$$

which implies

$$\boldsymbol{A}^- = -(\mathbf{R} + \sum_j \mathbf{C}_j^t \mathbf{Q}_j^{*-1} \mathbf{C}_j^*)^{-1} (\mathbf{R} - \sum_j \mathbf{C}_j^t \mathbf{Q}_j^{*-1} \mathbf{C}_j^*) \boldsymbol{A}^+ + 2(\mathbf{R} + \sum_j \mathbf{C}_j^t \mathbf{Q}_j^{*-1} \mathbf{C}_j^*)^{-1} \sum_i \mathbf{C}_i^t \boldsymbol{B}_i^-. \quad \text{(A17)}$$

When this expression is inserted in the lower expression in (A15) the following relation is obtained

$$\boldsymbol{B}_i^+ = \mathbf{Q}_i^{*-1} \mathbf{C}_i^* [\mathbf{I} + (\mathbf{R} + \sum_j \mathbf{C}_j^t \mathbf{Q}_j^{*-1} \mathbf{C}_j^*)^{-1} (\mathbf{R} - \sum_j \mathbf{C}_j^t \mathbf{Q}_j^{*-1} \mathbf{C}_j^*)] \boldsymbol{A}^+ + 2\mathbf{Q}_i^{*-1} \mathbf{C}_i^* (\mathbf{R} + \sum_j \mathbf{C}_j^t \mathbf{Q}_j^{*-1} \mathbf{C}_j^*)^{-1} \sum_k \mathbf{C}_k^t \boldsymbol{B}_k^- + \boldsymbol{B}_i^-. \quad \text{(A18)}$$

By introducing a scattering matrix, the linear system can be written as

$$\begin{pmatrix} \boldsymbol{A}^- \\ \boldsymbol{B}_1^+ \\ \vdots \\ \boldsymbol{B}_N^+ \end{pmatrix} = \begin{pmatrix} \mathbf{S}_{1,1}^{\mathrm{l}} & \mathbf{S}_{1,2}^{\mathrm{l}} & \cdots & \mathbf{S}_{1,N+1}^{\mathrm{l}} \\ \mathbf{S}_{2,1}^{\mathrm{l}} & \mathbf{S}_{2,2}^{\mathrm{l}} & \cdots & \mathbf{S}_{2,N+1}^{\mathrm{l}} \\ \vdots & \vdots & \ddots & \vdots \\ \mathbf{S}_{N+1,1}^{\mathrm{l}} & \mathbf{S}_{N+1,2}^{\mathrm{l}} & \cdots & \mathbf{S}_{N+1,N+1}^{\mathrm{l}} \end{pmatrix} \begin{pmatrix} \boldsymbol{A}^+ \\ \boldsymbol{B}_1^- \\ \vdots \\ \boldsymbol{B}_N^- \end{pmatrix}, \quad \text{(A19)}$$

where the elements of the scattering matrix are

$$\begin{cases} \mathbf{S}_{1,1}^{\mathrm{l}} = -(\mathbf{R} + \sum_j \mathbf{C}_j^t \mathbf{Q}_j^{*-1} \mathbf{C}_j^*)^{-1} (\mathbf{R} - \sum_j \mathbf{C}_j^t \mathbf{Q}_j^{*-1} \mathbf{C}_j^*), \\ \mathbf{S}_{1,i+1}^{\mathrm{l}} = 2(\mathbf{R} + \sum_j \mathbf{C}_j^t \mathbf{Q}_j^{*-1} \mathbf{C}_j^*)^{-1} \mathbf{C}_i^t, \\ \mathbf{S}_{i+1,1}^{\mathrm{l}} = \mathbf{Q}_i^{*-1} \mathbf{C}_i^* [\mathbf{I} + (\mathbf{R} + \sum_j \mathbf{C}_j^t \mathbf{Q}_j^{*-1} \mathbf{C}_j^*)^{-1} (\mathbf{R} - \sum_j \mathbf{C}_j^t \mathbf{Q}_j^{*-1} \mathbf{C}_j^*)], \\ \mathbf{S}_{i+1,i+1}^{\mathrm{l}} = 2\mathbf{Q}_i^{*-1} \mathbf{C}_i^* (\mathbf{R} + \sum_j \mathbf{C}_j^t \mathbf{Q}_j^{*-1} \mathbf{C}_j^*)^{-1} \mathbf{C}_i^t + \mathbf{I}. \\ \mathbf{S}_{i+1,k+1}^{\mathrm{l}} = 2\mathbf{Q}_i^{*-1} \mathbf{C}_i^* (\mathbf{R} + \sum_j \mathbf{C}_j^t \mathbf{Q}_j^{*-1} \mathbf{C}_j^*)^{-1} \mathbf{C}_k^t. \end{cases} \quad \text{(A20)}$$

This is the supercell correspondence of the single cell scattering matrix that is derived in [8]. The rest of the analysis used in [8] can now be applied.

REFERENCES

1. Eibert, T. F., J. L. Volakis, D. R. Wilton, and D. R. Jackson, "Hybrid FE/BI modeling of 3-D doubly periodic structures utilizing triangular prismatic elements and an MPIE formulation accelerated by the Ewald transformation," *IEEE Trans. Antennas Propagat.*, Vol. 47, No. 5, 843–850, May 1999.
2. Holter, H., "Analysis and design of broadband phased array antennas," Ph.D. thesis, Royal Institute of Technology, Division of Electromagnetic Theory, S-100 44 Stockholm, Sweden, 2000.
3. Kristensson, G., M. Åkerberg, and S. Poulsen, "Scattering from a frequency selective surface supported by a bianisotropic substrate," *Progress In Electromagnetics Research*, PIER 35, 83–114, 2002.
4. Kristensson, G., S. Poulsen, and S. Rikte, "Propagators and scattering of electromagnetic waves in planar bianisotropic slabs — an application to frequency selective structures," *Progress In Electromagnetics Research*, PIER 48, 1–25, 2004.
5. Sjöberg, D., "Coherent effects in single scattering and random errors in antenna technology," *Progress In Electromagnetics Research*, PIER 50, 13–39, 2005.
6. Tsao, C.-H. and R. Mittra, "Spectral-domain analysis of frequency selective surfaces comprised of periodic arrays of cross dipoles and Jerusalem crosses," *IEEE Trans. Antennas Propagat.*, Vol. 32, No. 5, 478–486, 1984.
7. Vardaxoglou, J. C., *Frequency Selective Surfaces (Analysis and Design)*, Research Studies Press, 1997.
8. Widenberg, B., S. Poulsen, and A. Karlsson, "Scattering from thick frequency selective screens," *Journal of Electromagnetic Wavesd Applicationd*, Vol. 14, No. 9, 1303–1328, 2000.